# Electrospun Hollow Nanofiber Surfaces as Dielectric Mediums for Highly Sensitive Flexible Capacitive Pressure Sensors in Low-Pressure Regimes

Shaharyar Siddique, Amit Barua, Rituporn Gogoi, and Vipul Sharma

***Abstract*—Flexible capacitive pressure sensors have gained significant attention in flexible electronics, offering extensive material and design options for various active sensing needs. Despite significant advances, achieving high sensitivity at very low pressures (<5 kPa) remains a challenge. Tailoring the dielectric layer is one of the most effective strategies to address this issue, with recent work showing that incorporating nanostructures can substantially improve sensor performance. Here, we employ coaxially electrospun hollow nanofibers characterized by a high surface-to-volume ratio, enhanced air gaps, and densely packed microstructure-nanostructure to fabricate a highly sensitive capacitive pressure sensor. Systematic characterization across varying pressure ranges revealed that the sensor achieved superior sensitivity in the low-pressure range (0.2–2 kPa), outperforming sensors fabricated using traditional electrospun nanofiber dielectric layers. In particular, the sensor exhibited a maximum sensitivity of 1.05 $kPa^{-1}$ at a pressure of 1 kPa. This performance gain is attributed to the hollow air core of the fibers, which improves dielectric properties by increasing surface area, roughness, deformability, and charge formation. However, the sensor's sensitivity reduces at higher pressures, ultimately falling below that of conventional single-shell fiber-based sensors due to the reduced influence of the air gaps within the hollow fibers. These findings highlight the potential of hollow fiber architectures for low-pressure-sensing applications while also highlighting opportunities for further optimization.**

***Index Terms*—Capacitive pressure sensor, coaxial electrospinning, dielectric layer, hollow nanofibers, sensitivity.**

## I. Introduction

THE rapid evolution of flexible electronics has stimulated the development of innovative sensors, especially in capacitive pressure sensing [1], [2], [3], [4], [5], [6], [7]. The sensitivity of these sensors depends on multiple factors, including the properties of the conductive surfaces, the dielectric material, and the spacing between conductive layers [7], [8], [9]. Traditional capacitive pressure sensors commonly employ dielectric layers made from planar surfaces with moderate dielectric properties, offering flexibility, ease of fabrication, and decent sensitivity. From a design perspective, sensor sensitivity can be enhanced by introducing nanostructures onto conductive surfaces, dielectric layers, or both [10], [11]. Electrospinning is widely used to fabricate nanostructured fibers [12], which exhibits a high surface-to-volume ratio [13], [14], porosity [15], [16], and tunable mechanical and electrical properties [17], [18]. Owing to these features, electrospun fibers are well-suited for applications in filtration, energy storage, and sensing technologies [17]. By applying a high voltage to a polymer solution, electrospinning enables the formation of continuous fibers with controlled morphology, diameter, and composition [19]. Recently, researchers have leveraged electrospun nanofibers for conductive layers and dielectric layers in pressure sensors [20], [21], [22]. Notably, traditional single-shell electrospun nanofibers can achieve good sensitivity in low-pressure regimes by increasing surface roughness at the microscale or nanoscale, which traps air and enhances the sensing response. However, this sensitivity can be further improved by employing hollow fibers, whose internal cavities provide additional dielectric benefits and reinforce capacitance changes under minimal loads.

To address these challenges, coaxial electrospinning, a modification of the conventional electrospinning technique enables the creation of more complex fiber architectures such as core-shell and hollow nanofibers [23], [24]. In coaxial electrospinning, two centrally aligned nozzles simultaneously dispense a core and a sheath solution, producing fibers with a tailored internal structure. This approach facilitates the fabrication of hollow fibers featuring an inner core and an outer shell, which significantly enhance dielectric properties compared to solid nanofibers. The inclusion of hollow geometries amplifies charge storage capacity, resulting in improved performance for precise pressure measurements in capacitive sensors [25]. Notably, the coaxial design offers substantial benefits in low-pressure regimes, where even subtle changes in pressure can be detected, a feat often unattainable by traditional single-shell fibers.

In this work, we present a comparative performance analysis of coaxially electrospun hollow fibers and single-shell fibers as the dielectric layer in capacitive pressure sensors. Sensor performance was evaluated in terms of sensitivity within the low-pressure range. Two pressure sensors were fabricated: one incorporating a hollow nanofiber surface as the dielectric layer

Received 11 May 2025; accepted 28 May 2025. Date of publication 5 June 2025; date of current version 31 July 2025. This work was supported in part by the KONE Foundation under Grant 202012035, in part by the Research Council of Finland under Grant 331368, and in part by the Project DURATRANS 2024–2027 through the Framework of M-ERA.Net under Grant 364364. *(Shaharyar Siddique and Amit Barua contributed equally to this work.) (Corresponding author: Vipul Sharma.)*

The authors are with the Department of Mechanical and Materials Engineering, University of Turku, 20014 Turku, Finland (e-mail: vipul.sharma@utu.fi).

This article has supplementary downloadable material available at https://doi.org/10.1109/JFLEX.2025.3577111, provided by the authors.

Digital Object Identifier 10.1109/JFLEX.2025.3577111

and the other incorporating a single-shell nanofiber surface. The single-shell nanofiber sensor (control) was characterized as a reference for comparison. Following characterization, the sensitivities of both sensors were analyzed and compared.

## II. Materials and Methods

### A. Materials

To prepare electrospun nanofibers, polycaprolactone (PCL) was purchased from Sigma Aldrich. Cellulose tape for encapsulation of capacitive sensors was purchased from 3M. Connecting wires were purchased from Farnell to fabricate electrical contacts of the capacitive sensor. Flexible ITO films (ITO on PET, sheet resistance 60 Ω/sq) used during the experiment were purchased from Sigma Aldrich. Solvents such as dimethylformamide (DMF) and dichloromethane (DCM) used during the experiments were purchased from Sigma Aldrich.

### B. Characterization

The electrospun nanofibers were produced using an electrospinning setup (Spinbox[1] by Bioinicia, Spain). Optical characterization was performed to initially check the formation of proper fibers without beads. Optical microscope (Euromex microscope iScope) was used in this case. High-resolution surface analysis of hollow nanofiber scaffold was performed using scanning electron microscope (SEM) (Thermo Scientific Inc., Eindhoven, The Netherlands) at 2 kV with an operating current of 25 pA. For cross-sectional characterization, the surface was soaked in a 2% PVA solution in water and then dried. Pressure sensor characterization was performed using a combined interface of a texture analyzer (TA.XT.plus100C, Stable Micro System) and inductance, capacitance, resistance (LCR) meter (GW-INSTEK LCR-6300). A texture analyzer (TA.XT.plus100C, Stable Micro System) equipped with a cylindrical probe with a diameter of 10 mm was used to apply and vary the pressure on the capacitive pressure sensors. The relative change in capacitance of the capacitive pressure sensor was measured using the LCR meter. A testing signal of 1 V at 1 kHz was employed for all measurements on the LCR meter.

### C. Electrospinning Procedure

Electrospinning was performed to produce single-shell nanofiber and hollow nanofibers with PCL. Single-shell or normal nanofibers is referred to as control nanofibers and the coaxially electrospun hollow nanofibers are referred to as hollow nanofibers. For electrospinning single-shell/control PCL fibers, a 12 wt% PCL solution was prepared by dissolving PCL (Mw 50 000) in DCM and DMF with a ratio of 1:1. The solution was stirred with a mechanical stirrer at 160-r/min overnight. The polymer solution was inserted into a 10-mL syringe; 15 kV of positive voltage was applied having a flow rate of 1.67 $\mu$L/min. A distance of 10 cm was fixed between the syringe needle and the collector throughout the electrospinning process for control fibers. For electrospinning hollow nanofibers, a 12 wt% PCL (Mw = 50 000) solution was prepared by dissolving PCL in DCM and DMF with a ratio of 4:1. The solution was stirred with the mechanical stirrer at 160-r/min overnight. The polymer solution was inserted in a 10-mL syringe connected to the syringe pump as a sheath. As a core material, silicone oil is chosen, which is connected to the pump using a separate 10-mL syringe; 15.5 kV of positive voltage was applied having a flow rate of 8 $\mu$L/min for the core material and 22 $\mu$L/min for the sheath material. A distance of 15 cm was maintained between the syringe needle and the collector throughout the electrospinning process for hollow fibers. Furthermore, the core needle had an inner diameter of 0.6 mm and the sheath needle had an inner diameter of 1.4 mm.

For control nanofibers, 12 wt% PCL solution in DCM and DMF (1:1) was prepared. Similarly, the solution was connected to a 10-mL syringe connected to a pump. The solution is pumped at the rate of 1.67 $\mu$L/min at an applied voltage of 15 kV having a collector distance of 10 cm. Moreover, all the electrospinning was operated at 22 °C. The nanofiber scaffolds were collected by peeling off the deposited layer from the aluminum foil and mounting the scaffold onto glass slides. Next, for postprocessing, the nanofiber scaffold was dipped into diethyl ether for 15 and 30 min subsequently to ensure the complete dissolution of silicone oil from the core to obtain hollow nanofiber scaffold. The prepared nanofiber film was heated at 45 °C for 1 h for drying properly.

### D. Device Fabrication

To fabricate the capacitive pressure sensor, fresh, flexible ITO films were used as the anode and cathode. The ITO films were cut into dimensions of $1.5 \times 3$ cm$^2$. The electrospun PCL nanofibers, following postprocessing, were carefully placed between the ITO films to serve as the dielectric layer. The stacked assembly was then securely encapsulated using cellulose tape. Copper wires were connected to both ends of the ITO films to provide electrical contacts.

## III. Results and Discussion

Fig. 1 presents a schematic overview of the complete fabrication process, detailing each step from the preparation of hollow nanofiber scaffolds to the assembly of the capacitive pressure sensor device. The process begins with the fabrication of hollow nanofibers using the electrospinning technique, which produces fibers with an enhanced surface-to-volume ratio, greater deformability, and hollow internal channels [23], [24], compared to traditional nanofibers (control nanofibers). The capacitive pressure sensor was designed with hollow nanofibers serving as the dielectric layer, aiming to improve sensitivity relative to sensors utilizing control nanofibers. Hollow PCL fibers were fabricated using the electrospinning method described in detail in Section II. In this process, silicone oil was used as the core material and PCL as the sheath material. Following electrospinning, the silicone oil was removed through a post-treatment process, resulting in hollow internal structures.

To evaluate the surface morphology of the nanofiber scaffold, high-resolution SEM was employed. The structural topography of both the control and hollow nanofibers was analyzed at varying magnifications, as shown in Fig. 2(a) and (b). SEM images of hollow fibers shown in Fig. 2(a) reveal the

[1]Registered trademark.

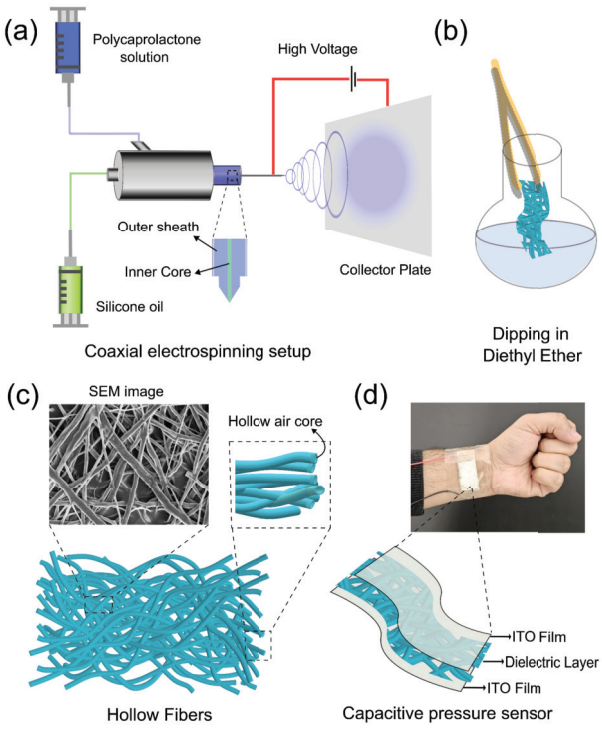


Fig. 1. Coaxially electrospun hollow nanofiber formation process and capacitive pressure sensor fabrication. (a) Coaxial electrospinning setup. (b) Dipping the electrospun nanofiber in diethyl ether to remove silicone oil from the core. (c) Formation of hollow fibers after removal of silicone oil. (d) Schematic of capacitive pressure sensor made with hollow fibers as dielectric and an image of real sensor attached to skin.

uniform deposition, with the inset image clearly illustrating the cross-sectional core-shell structure of the hollow nanofibers. The distinct color contrast, with brighter boundaries and darker cores, further supports the core-shell morphology. At higher magnifications, surface roughness on the coaxially electrospun fibers becomes visible, which can be attributed to minor defects on the fiber surface, as illustrated in the inset image of Fig. 2(a). Fiber diameter distribution analysis, as shown in Fig. 2(c), was conducted using SEM images of the control and coaxial hollow nanofibers in ImageJ software to evaluate fiber uniformity. The results indicate that the average diameter of the hollow fibers is 0.89 $\pm$ 0.05 $\mu$m, while the control fibers exhibit an average diameter of 0.43 $\pm$ 0.01 $\mu$m. The maximum diameter observed among the control fibers is approximately 0.6 $\mu$m, though such observations are relatively rare. In contrast, the hollow fibers exhibit diameters up to approximately 2 $\mu$m. This wider diameter indicates the hollow core present inside the hollow nanofibers. A comparison between the hollow fibers' and control fibers' properties is mentioned in Table S1 in the Supporting Information. However, it is noteworthy to mention that not all the fibers have uniform cores and shell thickness as evidenced in Fig. 2(a).

The presence of a hollow core in the nanofibers introduces an additional degree of deformation freedom, making these fibers ideal candidates for tactile sensing applications, particularly where high sensitivity is required in very low-

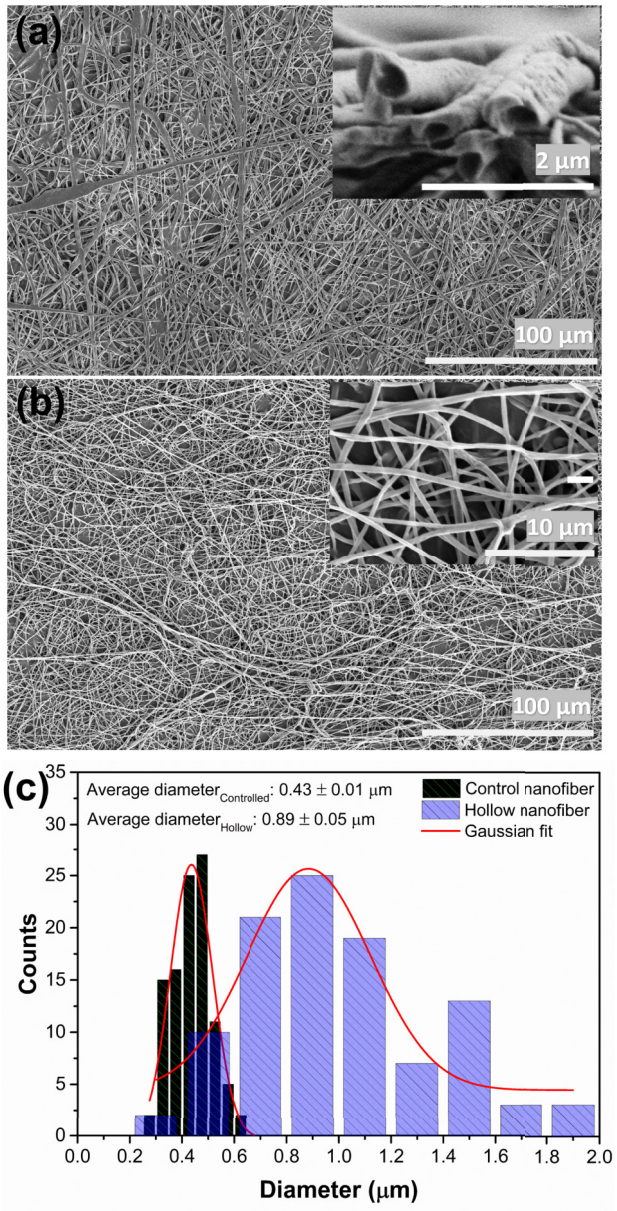


Fig. 2. SEM images of PCL hollow nanofibers and control nanofibers. (a) PCL hollow nanofibers. Inset shows the cross-sectional image of the hollow nanofibers. (b) PCL control nanofibers. Inset shows the magnified image of the control nanofibers. (c) Comparison of fiber diameter distribution between the hollow fibers and control fibers.

pressure regimes (<5 kPa). This structural feature significantly enhances the dielectric properties of hollow fibers compared to control fibers. The hollow air core within the hollow fibers contributes to increased compressibility and a higher capacitance response under low-pressure conditions. These observations highlight the potential of coaxially electrospun hollow fibers as superior dielectric materials compared to traditional single-shell electrospun fibers. The hollow structure enhances the effective dielectric constant due to the trapped air within the core, while the robust shell maintains structural integrity, ensuring durability, and resilience. Young's modulus ($E$) of neat, bulk PCL is 0.32–0.40 GPa at room temperature, according to the supplier's datasheet and published tensile

data. For electrospun PCL mats, the effective E decreases to 35–80 MPa because of fiber porosity and orientation; these values were used to estimate the mechanical compliance of the dielectric layer [26], [27]. A capacitive pressure sensor was fabricated using commercially available flexible ITO films as the conductive surfaces and electrospun PCL hollow fibers as the dielectric layer. The schematic of the sensor is shown in Fig. 1(d). The sensor operates by detecting pressure-induced changes within the active region through variations in capacitance. These changes in capacitance occur due to alterations in the distance between the two conductive surfaces as the applied pressure gradually increases.

To evaluate the performance of the pressure sensor, tests were conducted over a wide range of pressures. A texture analyzer equipped with a cylindrical probe (10 mm diameter) was used to apply pressure on the sensor. The analyzer was programmed using the Exponent Connect software provided with the instrument. Pressures ranging from very low values to higher levels (0.2–300 kPa) were incrementally applied to the sensor. The pressure was gradually increased over time, and the capacitance values were recorded using an LCR meter connected to the opposing ends of the sensor. The LCR meter was interfaced and programmed via MATLAB to record and visualize the capacitance data in real time.

Fig. 3(a) shows the digital image of the fabricated hollow fiber-based flexible capacitive pressure sensor. The test setup for pressure sensor characterization is depicted in Fig. 3(b). The change in relative capacitance with increasing pressure is shown in Fig. 3(c). At low pressures, the relative capacitance exhibits minimal variation, whereas at higher pressures, significant changes in capacitance are observed. The figure illustrates that the relative capacitance increases proportionally with the applied pressure. To analyze the $\Delta C/C_0$ behavior in the low-pressure regime, extensive data points were recorded for pressures below 1 kPa, as depicted in the inset of Fig. 3(c).

The sensitivity of the pressure sensor is presented in Fig. 3(d). Initially, the sensitivity increases with rising pressure, reaching a maximum value of 1.05 $kPa^{-1}$ at 1 kPa. Beyond this point, the sensitivity declines sharply with further pressure increase. The sensitivity was calculated using the following equation [28], [29]:

$$S = \frac{\Delta C/C_0}{\Delta P} \tag{1}$$

where $C_0$ is the initial capacitance, $\Delta C$ is the difference between the initial and final capacitance value, and $\Delta P$ is the pressure applied to the sensor.

A similar load-induced densification has been measured directly in electrospun mats by other groups. Choong et al. [30] and Silberstein et al. [31] observed >50% thickness loss by 100 kPa, followed by a mechanical plateau, while pressure-driven-flow tests showed a >60% decline in permeability between 5 and 140 kPa as porosity collapsed. This plateau coincides with the decline in sensitivity seen in Fig. 3(d), confirming that structural saturation—rather than electronic artifacts—governs the high-pressure response.

The two-region response in Fig. 3(d) mirrors trends reported for other porous dielectrics. Large-area reviews and targeted

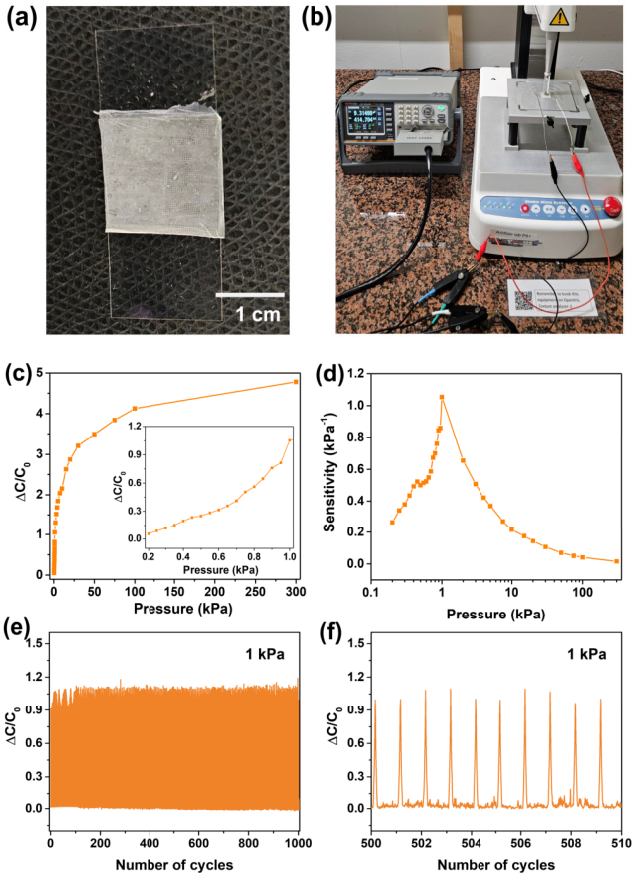


Fig. 3. Hollow nanofiber-based capacitive pressure sensor characterization. (a) Digital picture of hollow fiber-based flexible capacitive pressure sensor. (b) Test setup for pressure sensor characterization using texture analyzer and LCR meter. (c) Relative capacitance plotted as a function of pressure. Inset shows the magnified graph for lower pressure range. (d) Sensitivity of the pressure sensor. Three sensors have been tested and the graph represents the average of the results. (e) Cyclic test when dynamically loaded with 1-kPa pressure for 1000 cycles. (f) Magnified spectra of the cyclic test.

compression studies show that once air gaps inside a fibrous scaffold are largely eliminated (typically above ~40–80 kPa), further loading yields little extra densification and the device enters a "touch-mode" regime with much smaller $\Delta C/\Delta P$ [31], [32], [33]. Our sensitivity plateau above ~50 kPa is therefore consistent with complete or near-complete collapse of both the hollow fiber lumina and the interfiber voids.

A cyclic test was carried out for 1000 cycles to investigate the dynamic performance of the pressure sensor, focusing on factors like drift, stability of capacitance variation, and repeatability. The sensor was subjected to dynamic testing at a low-pressure condition of 1 kPa, with a cyclic frequency of 0.125 Hz. As presented in Fig. 3(e), the device demonstrated minor initial fluctuations in signal intensity, indicating minimal drift. Nevertheless, the overall performance remained consistent and repeatable throughout the prolonged operation. The magnified view of the sensor's signal intensity in Fig. 3(f) further highlights its stability under similar pressure conditions. The 1000-cycle test at 1 kPa [in Fig. 3(e)] exhibits around minimal signal drift, evidencing excellent elastic recovery of the hollow fiber dielectric even though

individual fibers may appear flattened under SEM vacuum conditions. In addition, cyclic tests were performed for different pressure values to check stability shown in Fig. S1 in the Supporting Information. PCL is a well-established hydrophobic and biodegradable polyester known for its environmental responsiveness. It remains structurally stable under abiotic or sterile conditions but undergoes hydrolysis in biologically active environments such as marine or composting systems [34], [35]. To extend operational lifetime while preserving biodegradability, strategies such as protective encapsulation or embedding with dormant enzymes have proven effective, enabling PCL-based systems to balance functional stability and sustainable degradation [36].

The step-wise response of the hollow fiber-based capacitive sensor was evaluated by applying a constant pressure of 1 kPa for a duration of 10 s, as illustrated in Fig. S2(a) in the Supporting Information. The sensor exhibited a stable change in capacitance throughout the period of applied pressure, demonstrating its capability for the consistent step-wise response. The response and recovery times, corresponding to the initiation and release of pressure, respectively, are highlighted in Fig. S2(b) and (c) in the Supporting Information. For an applied pressure of 1 kPa at a loading speed of 20 mm/s, the response time and recovery time were calculated to be ~84 and ~162 ms, respectively. Given that both response time and recovery time are influenced by the magnitude of applied pressure and speed, additional experiments were conducted using varying pressure and speed values. The corresponding results are presented as histograms in the Supporting Information [see Fig. S2(d) and (e)]. To compare the hollow fiber-based sensor with other recently developed flexible capacitive pressure sensors, we have included a comparison table (Table S2) in the Supporting Information. This table highlights key parameters such as materials, fabrication methods, sensitivity, response time, and pressure range.

To compare the performance of the PCL hollow nanofiber-based pressure sensor with the PCL control nanofiber-based pressure sensor, similar tests were conducted using the PCL control fiber-based device. A comparable pressure sensor was fabricated using ITO films; however, in this case, the dielectric layer was replaced with a single-shell control nanofiber that lacked the hollow air core present in the hollow fibers. The relative capacitance changes of the control sensor increased with applied pressure, displaying a similar trend to the hollow nanofiber-based sensor. The sensitivity of the control sensor was determined and compared to the previously characterized hollow nanofiber-based sensor, as shown in Fig. 4. The sensitivity of the control sensor peaked at 5 kPa with a value of 0.54 $kPa^{-1}$, which is significantly lower than the sensitivity of the hollow nanofiber-based sensor. The histogram in Fig. 4 illustrates that the hollow nanofiber-based pressure sensor demonstrated superior performance, with over 90% higher maximum sensitivity and greater efficiency in the low-pressure range (0.2–2 kPa). Three different sensors were tested with both the control and hollow nanofiber-based sensor. The histogram peaks represent the average sensitivity of the control and hollow fiber-based sensors, while the error bars indicate the corresponding standard deviations.

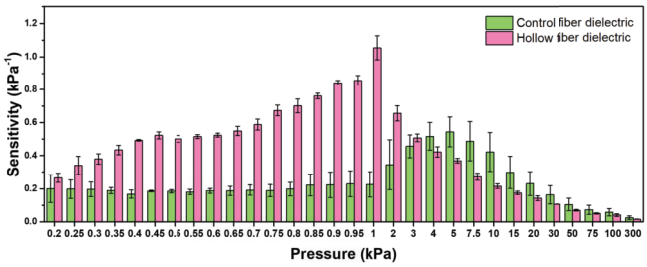


Fig. 4. Comparison of the sensitivity of the pressure sensor produced with hollow nanofibers and control nanofibers of PCL. The histogram peaks represent the average sensitivity and error bars show the standard deviation.

The superior performance of the hollow fibers as dielectric layers in the low-pressure range can also be attributed to the air-filled core, which acts as a compressible dielectric medium. This feature enhances the capacitance response under slight pressure variations, providing a significant advantage in sensitivity and efficiency. In contrast, the single shell/control fiber-based pressure sensor exhibits higher sensitivity compared to the hollow fiber-based pressure sensor at higher pressure values (4–300 kPa). This is possible because, beyond a certain load, the hollow structure is compressed due to pressure and no longer provides enhanced deformation anymore. In that case, the sensitivity of the pressure sensor having control fibers has more advantage due to their solid structure, which provides greater resistance to compression at higher stress. However, at low pressures, their limited deformability restricts the ability to respond sensitively to tiny pressure changes, resulting in lower sensitivity compared to hollow fibers. These observations confirm the suitability of hollow fibers as superior dielectric media compared to single fibers in pressure sensing at low-pressure regimes. The hollow structure enhances the dielectric properties due to the air core making it suitable for detecting tiny deformation, while the structural integrity of the shell ensures durability and resilience.

The pressure-sensing behavior can be approximated by modeling the dielectric layers in series, each contributing a distinct thickness ($d_i$) and permittivity ($\varepsilon_i$). For a hollow fiber network, we may separately account for the air inside the hollow core ($\varepsilon_{\text{in}}$, $d_{\text{in}}$), the fiber shell material ($\varepsilon_{\text{shell}}$, $d_{\text{shell}}$), and the air pockets between fibers ($\varepsilon_{\text{out}}$, $d_{\text{out}}$), as shown in Fig. 5.

Thus, the total capacitance $C_{\text{total}}$ can be written as

$$\frac{1}{C_{\text{total}}} = \frac{1}{C_{\text{in}}} + \frac{1}{C_{\text{shell}}} + \frac{1}{C_{\text{out}}}. \tag{2}$$

Equivalently, combining the denominators leads to

$$C_{\text{total}} = \frac{A}{\frac{d_{\text{in}}}{\varepsilon_{\text{in}}} + \frac{d_{\text{shell}}}{\varepsilon_{\text{shell}}} + \frac{d_{\text{out}}}{\varepsilon_{\text{out}}}}. \tag{3}$$

When the pressure is applied, the hollow core (inner air layer) compresses and may expel trapped air, reducing $d_{\text{in}}$ and altering $\varepsilon_{\text{in}}$. Likewise, the air pockets between fibers ($d_{\text{out}}$) undergo compression or deformation. At low pressures, the presence of air both inside and outside the fibers provides a large change in capacitance (high sensitivity) due to air's low

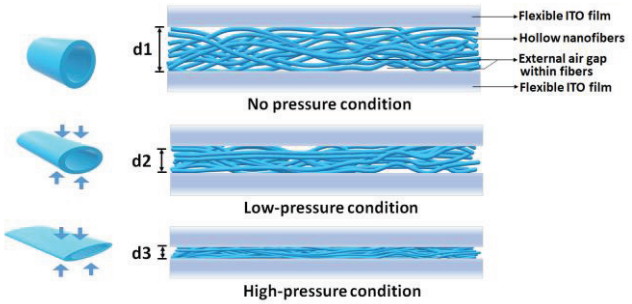


Fig. 5. Mechanism of the capacitive pressure sensor at no pressure, low-pressure, and high-pressure conditions.

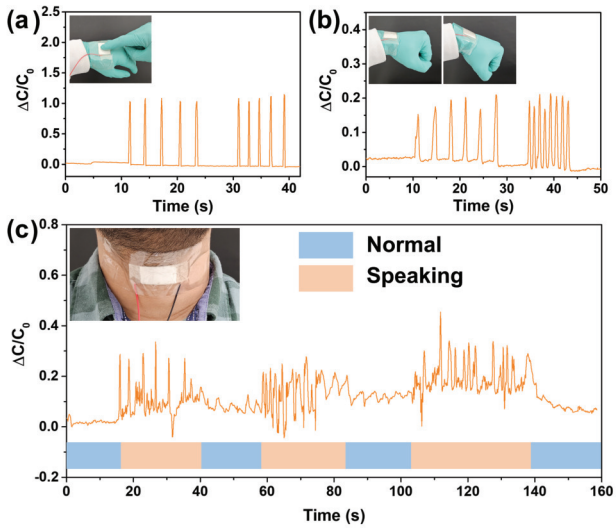


Fig. 6. Application demonstration of the hollow nanofiber-based capacitive pressure sensor. (a) Touch sensor application. (b) Wrist gesture movement detection. (c) Vocal cord movement detection during speaking.

dielectric constant ($\varepsilon_{\text{air}} \approx 1$) and the ease of deforming those hollow voids.

As the load increases, however, the hollow structures collapse and the air is partially expelled, reducing the overall advantage of the hollow design and leading to a decline in sensitivity at higher pressures. Equation (3) is used here as a qualitative framework. Similar series-void models have already been quantitatively validated for electrospun mats and microstructured dielectrics [28], [29], [31]. Those studies show that void collapse above ~5 kPa leads to a mechanical-electrical plateau exactly the variation observed in Fig. 3(d).

To showcase the potential of hollow fiber-based pressure sensor as an electronic skin (e-skin), it was tested in various real-world applications, including tactile sensing, human motion detection, and vocal cord vibration monitoring. Fig. 6(a)–(c) illustrates the hollow nanofiber-based sensor attached to different parts of the human body, effectively functioning as a tactile sensor. Fig. 6(a) demonstrates tactile sensing by placing the sensor on a human hand. Changes in relative capacitance ($\Delta C/C_0$) were observed for each touch, indicating the sensor's ability to detect tactile events. In Fig. 6(b), the sensor mounted on a human wrist shows consistent real-time changes in capacitance corresponding to wrist movements. Fig. 6(c) highlights variations in capacitance during vocal activities, such as speaking, compared to a resting state. Additionally, to demonstrate the sensor's applicability in the low-pressure range, an experiment was conducted with the sensor attached to the human throat during speaking and whispering (see Fig. S3). Speaking corresponds to higher pressure while whispering represents lower pressure. The sensor successfully detected subtle pressure changes in the throat muscles during whispering, highlighting its sensitivity to low-pressure variations. These findings confirm the sensor's suitability for real-time monitoring across a wide range of pressures and body movements, making it a promising candidate for medical applications (e.g., health monitoring devices, voice signal detection, and heart rate monitoring).

## IV. Conclusion

In summary, we have developed a highly sensitive capacitive pressure sensor utilizing coaxially electrospun hollow fibers as the dielectric medium. The sensor was systematically characterized under varying pressure loads to evaluate its sensing range, and cyclic tests were conducted to assess its reliability. Notably, the hollow fiber-based sensor exhibited superior sensitivity in the low-pressure range (0.2–2 kPa) compared to the sensor fabricated with traditional electrospun nanofibers as the dielectric layer. This enhanced sensitivity is attributed to the hollow air core within the hollow fiber network, which seems to improve dielectric properties by enhancing surface-to-volume ratio, surface roughness, enhanced deformability, and charge formation. However, while the sensor demonstrated excellent sensitivity at lower pressures, a decrease in sensitivity was observed at higher pressures, where its performance fell below that of capacitive sensors based on single-shell electrospun fibers. This suggests the diminishing effect of hollow air gaps with increasing pressure.

## Acknowledgment

The authors are thankful to the Materials Research Infrastructure (MARI) and Sustainable Fabrication (SusFab) at the University of Turku, Turku, Finland, for infrastructure facilities. They acknowledge Ermei Mäkilä from the Department of Physics and Astronomy, University of Turku, and Linda Broere from the Department of Mechanical and Materials Engineering, University of Turku, for their assistance with scanning electron microscope (SEM) analysis. Amit Barua is thankful to Tekniikan edistämissäätiö (TES) Foundation for encouragement support. The dataset/code used in this work is publicly available at Zenodo: https://doi.org/10.5281/zenodo.15581912

## References

[1] P. G. Reddy et al., "Sustainable cross-linked poly(glycerol–co–δ–valerolactone) urethane substrates and multipurpose transparent electrodes for wearable electronics," *Chem. Eng. J.*, vol. 495, Sep. 2024, Art. no. 153531, doi: 10.1016/j.cej.2024.153531.

[2] P. G. Reddy et al., "Biodegradable, self-adhesive, stretchable, transparent, and versatile electronic skins based on intrinsically hydrophilic poly(caproactone-urethane) elastomer," *Adv. Eng. Mater.*, vol. 26, no. 24, Dec. 2024, Art. no. 2401704, doi: 10.1002/adem.202401704.

[3] A. Koivikko, V. Lampinen, K. Yiannacou, V. Sharma, and V. Sariola, "Biodegradable, flexible and transparent tactile pressure sensor based on rubber leaf skeletons," *IEEE Sensors J.*, vol. 22, no. 12, pp. 11241–11247, Jun. 2022, doi: 10.1109/JSEN.2021.3078807.

[4] A. Elsayes, V. Sharma, K. Yiannacou, A. Koivikko, A. Rasheed, and V. Sariola, "Plant-based biodegradable capacitive tactile pressure sensor using flexible and transparent leaf skeletons as electrodes and flower petal as dielectric layer," *Adv. Sustain. Syst.*, vol. 4, no. 9, Sep. 2020, Art. no. 2000056, doi: 10.1002/adsu.202000056.

[5] A. Chortos, J. Liu, and Z. Bao, "Pursuing prosthetic electronic skin," *Nature Mater.*, vol. 15, no. 9, pp. 937–950, Sep. 2016, doi: 10.1038/NMAT4671.

[6] X. Wang, L. Dong, H. Zhang, R. Yu, C. Pan, and Z. L. Wang, "Recent progress in electronic skin," *Adv. Sci.*, vol. 2, no. 10, Oct. 2015, Art. no. 1500169, doi: 10.1002/advs.201500169.

[7] R. B. Mishra, N. El-Atab, A. M. Hussain, and M. M. Hussain, "Recent progress on flexible capacitive pressure sensors: From design and materials to applications," *Adv. Mater. Technol.*, vol. 6, no. 4, Apr. 2021, Art. no. 2001023, doi: 10.1002/admt.202001023.

[8] S. Pyo, J. Choi, and J. Kim, "Flexible, transparent, sensitive, and crosstalk-free capacitive tactile sensor array based on graphene electrodes and air dielectric," *Adv. Electron. Mater.*, vol. 4, no. 1, Jan. 2018, Art. no. 1700427, doi: 10.1002/aelm.201700427.

[9] T. Li et al., "Flexible capacitive tactile sensor based on micropatterned dielectric layer," *Small*, vol. 12, no. 36, pp. 5042–5048, Sep. 2016, doi: 10.1002/smll.201600760.

[10] N. Shao, J. Wu, X. Yang, J. Yao, Y. Shi, and Z. Zhou, "Flexible capacitive pressure sensor based on multi-walled carbon nanotube electrodes," *Micro Nano Lett.*, vol. 12, no. 1, pp. 45–48, Jan. 2017, doi: 10.1049/mnl.2016.0529.

[11] J. Qin et al., "Flexible and stretchable capacitive sensors with different microstructures," *Adv. Mater.*, vol. 33, no. 34, Aug. 2021, Art. no. 2008267, doi: 10.1002/adma.202008267.

[12] B. A. Chinnappan, M. Krishnaswamy, H. Xu, and M. E. Hoque, "Electrospinning of biomedical nanofibers/nanomembranes: Effects of process parameters," *Polymers*, vol. 14, no. 18, p. 3719, Sep. 2022, doi: 10.3390/polym14183719.

[13] G. Yazgan et al., "Steering surface topographies of electrospun fibers: Understanding the mechanisms," *Sci. Rep.*, vol. 7, no. 1, pp. 1–13, Mar. 2017, doi: 10.1038/s41598-017-00181-0.

[14] A. E. Fetz, C. A. Fantaziu, R. A. Smith, M. Z. Radic, and G. L. Bowlin, "Surface area to volume ratio of electrospun polydioxanone templates regulates the adsorption of soluble proteins from human serum," *Bioengineering*, vol. 6, no. 3, p. 78, Aug. 2019, doi: 10.3390/bioengineering6030078.

[15] N. Asano, S. Sugihara, S. Suye, and S. Fujita, "Electrospun porous nanofibers with imprinted patterns induced by phase separation of immiscible polymer blends," *ACS Omega*, vol. 7, no. 23, pp. 19997–20005, Jun. 2022, doi: 10.1021/acsomega.2c01798.

[16] F. Zhang, Y. Si, J. Yu, and B. Ding, "Electrospun porous engineered nanofiber materials: A versatile medium for energy and environmental applications," *Chem. Eng. J.*, vol. 456, Jan. 2023, Art. no. 140989, doi: 10.1016/j.cej.2022.140989.

[17] Y. Wang, T. Yokota, and T. Someya, "Electrospun nanofiber-based soft electronics," *NPG Asia Mater.*, vol. 13, no. 1, pp. 1–22, Mar. 2021, doi: 10.1038/s41427-020-00267-8.

[18] W. Serrano-Garcia, I. Bonadies, S. W. Thomas, and V. Guarino, "New insights to design electrospun fibers with tunable electrical conductive–semiconductive properties," *Sensors*, vol. 23, no. 3, p. 1606, Feb. 2023, doi: 10.3390/s23031606.

[19] P. Rathore and J. D. Schiffman, "Beyond the single-nozzle: Coaxial electrospinning enables innovative nanofiber chemistries, geometries, and applications," *ACS Appl. Mater. Interfaces*, vol. 13, no. 1, pp. 48–66, Jan. 2021, doi: 10.1021/acsami.0c17706.

[20] M. Ren et al., "A wearable and high-performance capacitive pressure sensor based on a biocompatible PVP nanofiber membrane via electrospinning and UV treatment," *J. Mater. Chem. C*, vol. 10, no. 29, pp. 10491–10499, Jul. 2022, doi: 10.1039/d2tc00955b.

[21] Y. Zhu et al., "A flexible capacitive pressure sensor based on an electrospun polyimide nanofiber membrane," *Organic Electron.*, vol. 84, Sep. 2020, Art. no. 105759, doi: 10.1016/j.orgel.2020.105759.

[22] R. Li, M. Panahi-Sarmad, T. Chen, A. Wang, R. Xu, and X. Xiao, "Highly sensitive and flexible capacitive pressure sensor based on a dual-structured nanofiber membrane as the dielectric for attachable wearable electronics," *ACS Appl. Electron. Mater.*, vol. 4, no. 1, pp. 469–477, Jan. 2022, doi: 10.1021/acsaelm.1c01098.

[23] M. Lallave et al., "Filled and hollow carbon nanofibers by coaxial electrospinning of alcell lignin without binder polymers," *Adv. Mater.*, vol. 19, no. 23, pp. 4292–4296, Dec. 2007, doi: 10.1002/adma.200700963.

[24] Y.-C. Chiang, W.-T. Chin, and C.-C. Huang, "The application of hollow carbon nanofibers prepared by electrospinning to carbon dioxide capture," *Polymers*, vol. 13, no. 19, p. 3275, Sep. 2021, doi: 10.3390/polym13193275.

[25] M. A. Haghighat Bayan, F. Afshar Taromi, M. Lanzi, and F. Pierini, "Enhanced efficiency in hollow core electrospun nanofiber-based organic solar cells," *Sci. Rep.*, vol. 11, no. 1, p. 21144, Oct. 2021, doi: 10.1038/s41598-021-00580-4.

[26] M. A. Woodruff and D. W. Hutmacher, "The return of a forgotten polymer–Polycaprolactone in the 21st century," *Prog. Polym. Sci.*, vol. 35, no. 10, pp. 1217–1256, Oct. 2010, doi: 10.1016/j.progpolymsci.2010.04.002.

[27] S. R. Baker, S. Banerjee, K. Bonin, and M. Guthold, "Determining the mechanical properties of electrospun poly-ε-caprolactone (PCL) nanofibers using AFM and a novel fiber anchoring technique," *Mater. Sci. Eng., C*, vol. 59, pp. 203–212, Feb. 2016, doi: 10.1016/j.msec.2015.09.102.

[28] R. Qin et al., "A new strategy for the fabrication of a flexible and highly sensitive capacitive pressure sensor," *Microsyst. Nanoeng.*, vol. 7, no. 1, pp. 1–12, Nov. 2021, doi: 10.1038/s41378-021-00327-1.

[29] H. Tian et al., "A sensitivity-optimized flexible capacitive pressure sensor with cylindrical ladder microstructural dielectric layers," *Sensors*, vol. 23, no. 9, p. 4323, Apr. 2023, doi: 10.3390/s23094323.

[30] L. T. Choong, M. M. Mannarino, S. Basu, and G. C. Rutledge, "Compressibility of electrospun fiber mats," *J. Mater. Sci.*, vol. 48, no. 22, pp. 7827–7836, Jun. 2013, doi: 10.1007/s10853-013-7528-x.

[31] M. N. Silberstein, C.-L. Pai, G. C. Rutledge, and M. C. Boyce, "Elastic–plastic behavior of non-woven fibrous mats," *J. Mech. Phys. Solids*, vol. 60, no. 2, pp. 295–318, Feb. 2012, doi: 10.1016/j.jmps.2011.10.007.

[32] H. Yuan et al., "Progress and challenges in flexible capacitive pressure sensors: Microstructure designs and applications," *Chem. Eng. J.*, vol. 485, Apr. 2024, Art. no. 149926, doi: 10.1016/j.cej.2024.149926.

[33] W. H. Ko and Q. Wang, "Touch mode capacitive pressure sensors," *Sens. Actuators A, Phys.*, vol. 75, no. 3, pp. 242–251, Jun. 1999, doi: 10.1016/S0924-4247(99)00069-2.

[34] M. Suzuki, Y. Tachibana, and K.-I. Kasuya, "Biodegradability of poly(3-hydroxyalkanoate) and poly(ε-caprolactone) via biological carbon cycles in marine environments," *Polym. J.*, vol. 53, no. 1, pp. 47–66, Jan. 2021, doi: 10.1038/s41428-020-00396-5.

[35] A. Heimowska, M. Morawska, and A. Bocho-Janiszewska, "Biodegradation of poly(ε-caprolactone) in natural water environments," *Polish J. Chem. Technol.*, vol. 19, no. 1, pp. 120–126, Mar. 2017, doi: 10.1515/pjct-2017-0017.

[36] N. K. Kalita, D. Hazarika, R. K. Srivastava, and M. Hakkarainen, "Faster biodegradable and chemically recyclable polycaprolactone with embedded enzymes: Revealing new insights into degradation kinetics," *Chem. Eng. J.*, vol. 496, Sep. 2024, Art. no. 153982, doi: 10.1016/j.cej.2024.153982.

**Shaharyar Siddique** received the B.Sc. degree in metallurgical and materials engineering from the University of Engineering and Technology, Lahore, Pakistan, in 2019. He is currently pursuing the master's degree in materials engineering technology with the University of Turku, Turku, Finland.

He is currently working at the Materials for Flexible Devices Group, University of Turku. His research interest encompasses nanofabrication techniques for designing electronic sensors.

**Amit Barua** received the M.Sc. degree in electronics engineering from the University of Southern Denmark, Sønderborg, Denmark, in 2022. He is currently pursuing the Ph.D. degree with the Materials Engineering Department, University of Turku, Turku, Finland.

He is working with the Materials for Flexible Devices Group, University of Turku. His research interests include the design and fabrication of bioinspired electronic sensors.

**Rituporn Gogoi** received the Ph.D. degree in chemical sciences from IIT Mandi, Mandi, India, in 2023.

In 2021, he received the SPARC Fellowship based on an Indo-French grant and was invited as a Visiting Researcher at Université Paris-Saclay, Orsay, France. Currently, he is investigating the field of functional 1-D and 2-D nanomaterials, with a particular focus on their application in highly flexible wearable electronic devices at the University of Turku, Turku, Finland.

**Vipul Sharma** received the Ph.D. degree in chemistry from IIT Mandi, Mandi, India, in 2018.

From 2018 to 2023, he was a Post-Doctoral Researcher at Tampere University, Tampere, Finland. Since 2023, he has been an Assistant Professor with the Department of Mechanical and Materials Engineering, University of Turku, Turku, Finland. His research focuses on novel materials, particularly 2-D and metal nanomaterials, sustainable polymers, bioinspired architectures, and the development of microfabrication-nanofabrication techniques to create flexible surfaces with useful functionalities.